J. Fluid Mech. (1967), *vol.* 29, *part* 2, *pp.* 391–399
Printed in Great Britain

Laminar free convection in boundary layers near horizontal cylinders and vertical axisymmetric bodies

By D. A. SAVILLE† AND S. W. CHURCHILL
Department of Chemical and Metallurgical Engineering, University of Michigan, Ann Arbor, Michigan

(Received 12 September 1966)

In this article the problem of describing free convection near either horizontal cylinders or vertical axisymmetric bodies with fairly arbitrary body contours is studied. The solutions of two, coupled, partial differential equations, for the temperature and stream functions, are represented by series which are universal with respect to body contours within a specified class of body shapes (e.g. round-nosed cylinders). The series appear to converge rapidly so that a minimum of computational effort is required, even for classes of body shapes which do not admit the usual similarity transformations. For either horizontal, circular cylinders or spheres the series converge faster than expansions of the Blasius type and one-term approximations compare favourably with some of the existing experimental data.

1. Introduction

Only a few studies of temperature-driven, laminar, free convection around submerged objects have dealt with the influence of the shape of the object. Of course, the asymptotic behaviour of the relationship between the Nusselt, Grashof, and Prandtl numbers can be ascertained from the differential equations alone at large Grashof numbers and large or small Prandtl numbers (e.g. Morgan & Warner 1956; Lefevre 1957; Hellums & Churchill 1960). The relations are:

$$\mathrm{Nu} \propto (\mathrm{Gr}\,\mathrm{Pr})^{\frac{1}{4}} \text{ for } \mathrm{Pr} \to \infty \quad \text{and} \quad \mathrm{Nu} \propto (\mathrm{Gr}\,\mathrm{Pr}^2)^{\frac{1}{4}} \quad \text{for} \quad \mathrm{Pr} \to 0.$$

Moreover, the proportionality function, which depends on the shape of the object, can be obtained in an explicit form for large Prandtl numbers (Acrivos 1962). However, at intermediate and small Prandtl numbers the effect of the body shape cannot be accounted for without a more extensive analysis.

In some cases where the body shape is simple (e.g. a vertical plate or cone), the partial differential equations describing the conservation of mass, momentum and energy can be reduced to two ordinary differential equations using similarity transformations. Numerical methods (Ostrach 1953) or the von Kármán–Pohlhausen integral method (Merk & Prins 1954; Braun, Ostrach & Heighway 1961) have been used to define the effects of the Prandtl number. On the other hand, in instances where the body shape precludes the use of similarity trans-

† Now at Shell Development Company, Emeryville, California.

formations (e.g. horizontal cylinders or spheres), integral methods (Merk & Prins 1954) and series expansion methods similar to the Blasius series for forced convection have been used (Chaing & Kaye 1962; Chaing, Ossin & Tien 1964). In almost all of these studies the *modus operandi* has been to ascertain the effect of the Prandtl number given a body contour. An exception is the work by Braun *et al.*, where the classes of body contours admitting similarity transformations were found.

It is apparent that none of the techniques mentioned so far accounts for the effects of body shape in a general manner. Hence, in the analysis to follow, new independent variables and series representations of the dependent variables will be introduced which are 'universal' with respect to the body contour. The choice of independent variables and series expansions is patterned after the work of Goertler (1957) on forced convection, since, in addition to their universal character, the first term in Goertler's series proved to be an excellent approximation for the flow around a circular cylinder at stations rather far from the stagnation point. Hence, this leads us to expect that the computational effort necessary to describe free convection around horizontal cylinders or spheres may be reduced to the order of magnitude of that required for the vertical plate. This economy would be of considerable importance in, for example, studies of free convection driven by both temperature and composition gradients since in this case there are five dimensionless parameters governing the phenomena.

If interfacial velocity effects are ignored, then free convection driven solely by composition gradients in the fluid can be described by using an analogy with temperature-driven convection. These interfacial velocity effects, which may or may not be small, have been studied by Acrivos (1962) and will not be considered here.

2. Development of basic equations

We begin the formal development with the familiar boundary-layer description of laminar, free convection around a submerged object. The surface of the object is assumed to be isothermal and the properties of the fluid surrounding the object will be taken as constants, excepting the density in the 'buoyancy term'. The equation expressing the conservation of thermal energy in terms of the dimensionless temperature and stream functions is

$$\mathrm{Pr}\,(\psi_y \Theta_x - \psi_x \Theta_y) = \Theta_{yy}. \tag{1}$$

The equation for the stream function ψ, for planar, two-dimensional flows, is

$$\psi_y \psi_{xy} - \psi_x \psi_{yy} = S(x)\,\Theta + \psi_{yyy}, \tag{2}$$

while for axisymmetric, two-dimensional flows it is

$$\frac{1}{r^2}(\psi_y \psi_{xy} - \psi_x \psi_{yy}) - \frac{r_x}{r^3}(\psi_y)^2 = S(x)\,\Theta + \frac{1}{r}\,\psi_{yyy}. \tag{3}$$

The equations are written in terms of the usual dimensionless and 'stretched' variables, and the subscripts denote differentiation with respect to the variable

indicated. If the characteristic length is denoted by L and distances along the surface by x_1 and normal to the surface by x_2, then

$$x = x_1/L, \quad y = x_2 \mathrm{Gr}^{\frac{1}{4}}/L, \tag{4}$$

where Gr denotes the Grashof number, $g\beta(\theta_s - \theta_\infty)L^3/\nu^2$. The kinematic viscosity is ν, the coefficient of thermal expansion β, the temperature of the surface θ_s, the temperature of the fluid far from the surface θ_∞, and g denotes the magnitude of the 'body force' vector (gravity in the usual case). Similarly, the Prandtl number, Pr, is the ratio of the kinematic viscosity ν to the thermal diffusivity α, and Θ is the dimensionless temperature, $(\theta - \theta_\infty)/(\theta_s - \theta_\infty)$. The sine of the angle between the body force vector and a normal to the surface of the object is $S(x)$, while r is the dimensionless radius of revolution for axisymmetric bodies, a function of x alone.

The stream function for planar, two-dimensional flows is defined in terms of the velocity components in the x_1 and x_2 directions by

$$u_1 = \frac{\nu}{L}\mathrm{Gr}^{\frac{1}{2}}\psi_y, \quad u_2 = -\frac{\nu}{L}\mathrm{Gr}^{\frac{1}{4}}\psi_x, \tag{5}$$

and for axisymmetric flows by

$$u_1 = \frac{\nu}{Lr}\mathrm{Gr}^{\frac{1}{2}}\psi_y, \quad u_2 = -\frac{\nu}{Lr}\mathrm{Gr}^{\frac{1}{4}}\psi_x. \tag{6}$$

The boundary conditions are:

(a) at the surface, $y = 0$,

$$\Theta = 1, \quad \psi_x = \psi_y = 0, \tag{7}$$

(b) far from the surface, $y \to \infty$,

$$\Theta = \psi_y = 0. \tag{8}$$

It is understood that the model, as presented, embodies several implicit restrictions. These are principally, that the surface is smooth enough and the Grashof number is large so that the boundary-layer equations are valid.

Our first step is to transform (3) into a form similar to that for planar flows. Hence, the following variables are introduced (cf. Mangler 1948)

$$\left.\begin{aligned} \hat{x} &= \int_0^x [r(z)]^2 dz, \\ \hat{y} &= ry, \\ \hat{\psi}_{\hat{y}} &= \frac{1}{r}\psi_y, \\ -\hat{\psi}_{\hat{x}} &= -\frac{1}{r^2}\psi_x + \frac{r_x}{r^3} y\psi_y. \end{aligned}\right\} \tag{9}$$

In terms of these variables the equation for the axisymmetric stream function is

$$r^2(\hat{\psi}_{\hat{y}}\hat{\psi}_{\hat{x}\hat{y}} - \hat{\psi}_{\hat{x}}\hat{\psi}_{\hat{y}\hat{y}}) = S(\hat{x})\,\Theta + r^2\hat{\psi}_{\hat{y}\hat{y}\hat{y}}. \tag{10}$$

The boundary conditions and the equation for the temperature function, Θ, are unchanged, except for the substitution of $\hat{\psi}$ for ψ, $\hat{x}$ for x, etc. Henceforth, the

'caret' notation will be understood implicitly. Now, based on arguments similar to those discussed by Goertler (1957), we introduce the transformations

$$\left.\begin{aligned}
\xi &= \int_0^x [S(z)]^{\frac{1}{3}}\,dz \quad \text{(planar flows)},\\
\xi &= \int_0^x [r(z)]^{-\frac{2}{3}}[S(z)]^{\frac{1}{3}}\,dz \quad \text{(axisymmetric flows)},\\
\eta &= (\tfrac{3}{4})^{\frac{1}{4}}\frac{y[S(x)]^{\frac{1}{3}}}{\xi^{\frac{1}{4}}} \quad \text{(planar flows)},\\
\eta &= (\tfrac{3}{4})^{\frac{1}{4}}\frac{y[S(x)]^{\frac{1}{3}}}{\xi^{\frac{1}{4}}[r(x)]^{\frac{2}{3}}} \quad \text{(axisymmetric flows)},\\
\psi(x,y) &= (\tfrac{4}{3})^{\frac{3}{4}}\xi^{\frac{3}{4}}F(\xi,\eta),\\
\theta(x,y) &= T(\xi,\eta).
\end{aligned}\right\} \tag{11}$$

The dependence of $F(\xi,\eta)$ and $T(\xi,\eta)$ on the Prandtl number is also to be understood implicitly. Using these transformations, (1), (2) and (10) become

$$\tfrac{4}{3}\xi(F_\eta T_\xi - F_\xi T_\eta) - FT_\eta = \frac{1}{\mathrm{Pr}}T_{\eta\eta}, \tag{12}$$

$$\tfrac{4}{3}\xi(F_\eta F_{\xi\eta} - F_\xi F_{\eta\eta}) - FF_{\eta\eta} + \tfrac{4}{3}K(\xi)F_\eta F_\eta = T + F_{\eta\eta\eta}, \tag{13}$$

where

$$\left.\begin{aligned}
K(\xi) &= \frac{1}{2} + \frac{1}{3}\frac{\xi}{S(\xi)}\frac{dS}{d\xi} \quad \text{(planar flows)},\\
K(\xi) &= \frac{1}{2} + \frac{1}{3}\frac{\xi[r(\xi)]^2}{S(\xi)}\frac{d(S/r^2)}{d\xi} \quad \text{(axisymmetric flows)}.
\end{aligned}\right\} \tag{14}$$

The boundary conditions are

$$T(\xi,0) = 1, \quad F(\xi,0) = F_\eta(\xi,0) = F_\eta(\xi,\infty) = T(\xi,\infty) = 0. \tag{15}$$

Goertler's (1957) terminology, of 'principal function' for $K(\xi)$, will be employed here. We note in passing that the condition for the existence of similarity transformations is that the principal function be a constant. The principal function can be expanded as the following series

$$K(\xi) = \sum_{=0}^{\infty} K_j \xi^{\alpha j}, \tag{16}$$

where α is a rational number. The numbers K_0 and α depend only on the class of the body shape, not on details of the contour. The analysis for the remainder of the terms in the expansion is straightforward and one finds: (1) for round-nosed axisymmetric bodies $K_0 = \frac{3}{8}$, $\alpha = \frac{3}{4}$; (2) for sharp-nosed cylinders $K_0 = \frac{1}{2}$, $\alpha = 1$; and (3) for round-nosed cylinders $K_0 = \frac{3}{4}$, $\alpha = \frac{3}{2}$.

For the circular cylinder

$$K(\xi) = \tfrac{3}{4} - (\tfrac{3}{40})(\tfrac{64}{27})^{\frac{1}{2}}\xi^{\frac{3}{2}} + \ldots, \tag{17}$$

a result which will be used in a later section, where the results for the circular cylinder are compared with experimental data.

Now, having shown the form of the expansion for the principal function, we introduce the following expansions for the other dependent variables

$$F(\xi,\eta)=\sum_{j=0}^{\infty}F_j(\eta)\xi^{\alpha j},\quad T(\xi,\eta)=\sum_{j=0}^{\infty}T_j(\eta)\xi^{\alpha j}. \tag{18}$$

In terms of the new variables we have

(*a*) for $j=0$

$$F_0'''+F_0F_0''-\tfrac{4}{3}K_0F_0'F_0'+T_0=0, \tag{19}$$

$$T_0''+\Pr F_0T_0'=0, \tag{20}$$

(*b*) for $j=1,2,3\ldots$

$$\left.\begin{aligned}&F_j'''+F_0F_j''-\tfrac{4}{3}(\alpha j+2K_0)F_0'F_j'+(\tfrac{4}{3}\alpha j+1)F_0''F_j-\tfrac{4}{3}K_jF_0'F_0'+T_j=RF_j,\\&RF_j\overset{\mathrm{d}}{=}\sum_{k=1}^{j-1}\left\{\tfrac{4}{3}(\alpha k+K_0)F_k'F_{j-k}'-(\tfrac{4}{3}\alpha k+1)F_kF_{j-k}'+\tfrac{4}{3}K_{j-k}\sum_{i=0}^{k}F_i'F_{k-i}'\right\},\end{aligned}\right\} \tag{21}$$

$$\left.\begin{aligned}&T_j''+\Pr F_0T_j'-\tfrac{4}{3}\alpha j\Pr F_0'T_j+(\tfrac{4}{3}\alpha j+1)\Pr F_jT_0'=RT_j,\\&RT_j\overset{\mathrm{d}}{=}\Pr\sum_{k=1}^{j-1}\{\tfrac{4}{3}\alpha kT_kF_{j-k}'-(\tfrac{4}{3}\alpha k+1)F_kT_{j-k}'\}.\end{aligned}\right\} \tag{22}$$

The boundary conditions are:

(*a*) for $j=0$

$$T_0(0)=1,\quad F_0(0)=F_0'(0)=T_0(\infty)=F_0'(\infty)=0, \tag{23}$$

(*b*) for $j=1,2,3$

$$T_j(0)=F_j(0)=F_j'(0)=T_j(\infty)=F_j'(\infty)=0. \tag{24}$$

Equations (19) and (20), along with their boundary conditions, comprise the same system as that studied by Ostrach (1953) for the vertical plate ($K_0=\frac{1}{2}$, $\alpha=1$). The succeeding systems of equations ($j=1,2,3,\ldots$) are linear and, owing to the form of the equations, the coefficients in the expansion of the principal function (the K_j's) can be scaled out of the systems. For example, if new variables for $j=1$ are defined as

$$T_1(\eta)=K_1t_1(\eta)\quad F_1(\eta)=K_1f_1(y), \tag{25}$$

then K_1 no longer appears in the differential equation for $j=1$. A similar procedure is possible for the higher-order terms ($j=2,3,\ldots$), although the algebra is rather tedious. Thus, it is possible to describe free convection around all objects of a given class of body shapes in terms of ordinary differential equations in which the parameters particular to a body contour are absent. Hence, for a particular class of body shapes and specific Prandtl number the differential equations can be solved once and for all. Then the resulting solutions can be applied to any body contour within the class by simply assembling the series. Furthermore, as demonstrated in the next section, the series converge rapidly enough in some instances so that only a few terms need be calculated. Indeed, it will turn out that only one term is needed for the horizontal cylinder for most purposes.

We close this section with a definition of the Nusselt number to be used later:

$$\mathrm{Nu}\overset{\mathrm{d}}{=}\frac{\text{(heat flux density) (characteristic length)}}{\text{(thermal conductivity) (temperature difference)}},$$

or

$$\mathrm{Nu}\overset{\mathrm{d}}{=}-\mathrm{Gr}^{\frac{1}{4}}\Theta_y(0). \tag{26}$$

3. Applications of the series

In this section we shall present some results obtained from numerical solutions of a few of the equations developed in the previous section. These results are compared with experimental data taken from the literature and with results obtained by other methods. Of course the differential equations for the zero-order terms have already been solved by numerical methods to describe free convection near planar, sharp-nosed bodies and the results are in substantial

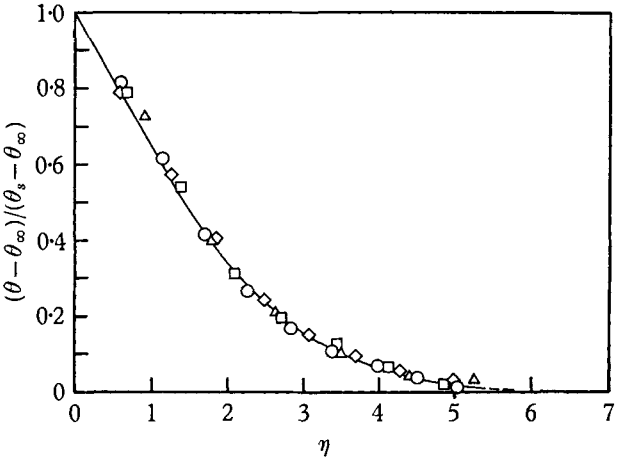

FIGURE 1. Temperature-driven free convection around a horizontal, circular cylinder. Dimensionless temperature against dimensionless normal distance at 90° from the lower stagnation point. Experimental data of Jodlbauer, Pr = 0·7: ○, Gr = 7×10^5; □, Gr = $1{\cdot}6\times10^5$; ◇, Gr = $9{\cdot}3\times10^4$; △, Gr = $9{\cdot}4\times10^3$. Series representation: ——, one or two terms.

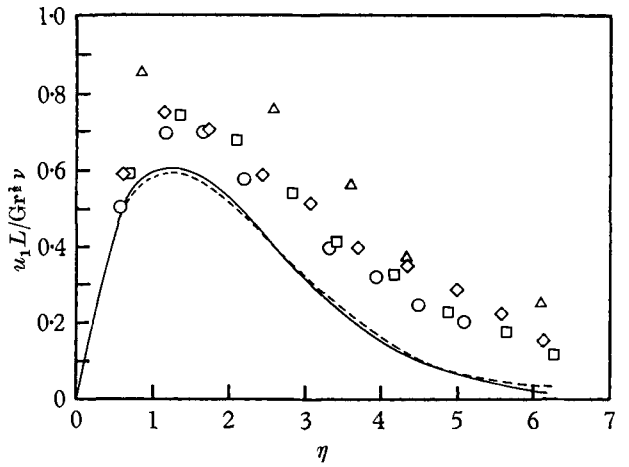

FIGURE 2. Temperature-driven free convection around a horizontal, circular cylinder. Dimensionless tangential velocity against dimensionless normal distance at 90° from the lower stagnation point. Experimental data of Jodlbauer, Pr = 0·7: ○, Gr = 7×10^5; □, Gr = $1{\cdot}6\times10^5$; ◇, Gr = $9{\cdot}3\times10^3$; △, Gr = $9{\cdot}4\times10^3$. Series representation: — —, one term; —, two term.

agreement with the existing experimental data (Schmidt & Beckmann 1930; Ostrach 1953). The transformations and series representations were chosen in order to describe, with a minimum of effort, free convection near objects having body contours which do not admit of similarity transformations. Hence, in order to test this facility, we first examine the results for circular cylinders.

For Pr = 0·7, the derivatives of the zero- and first-order terms, evaluated at the surface, were found to be $T_0'(0) = -0{\cdot}3702$, $F_0''(0) = 0{\cdot}8593$, $T_1'(0) = -0{\cdot}03226K_1$ and $F_1''(0) = -0{\cdot}09149K_1$. Series representations of the velocity tangent to the surface and the temperature together with some experimental data

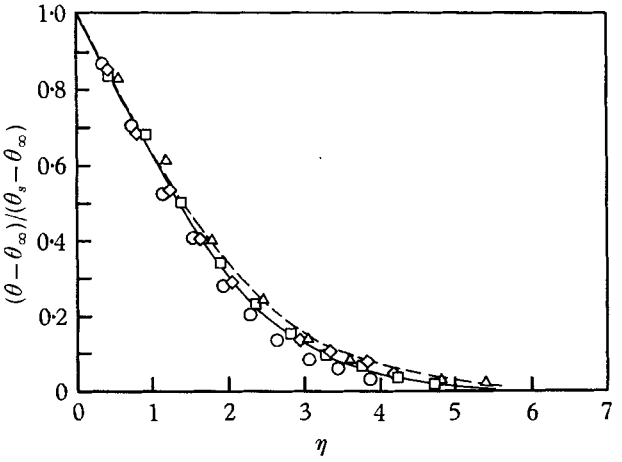

FIGURE 3. Temperature-driven free convection around a horizontal, circular cylinder. Dimensionless temperature against dimensionless normal distance at 150° from the lower stagnation point. Experimental data of Jodlbauer, Pr = 0·7: ○, Gr = 7×10^5; □, Gr = $1{\cdot}6\times10^5$; ◇, Gr = $9{\cdot}3\times10^4$; △, Gr = $9{\cdot}4\times10^3$. Series representation: — —, one term; —, two term.

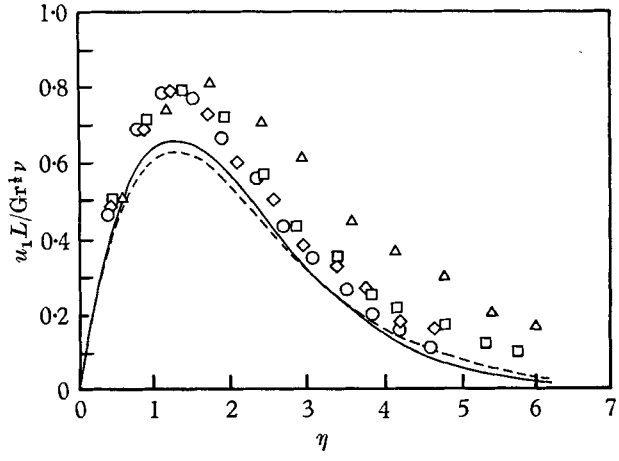

FIGURE 4. Temperature-driven free convection around a horizontal, circular cylinder. Dimensionless tangential velocity against dimensionless normal distance at 150° from the lower stagnation point. Experimental data of Jodlbauer, Pr = 0·7: ○, Gr = 7×10^5; □, Gr = $1{\cdot}6\times10^5$; ◇, Gr = $9{\cdot}3\times10^4$; △, Gr = $9{\cdot}4\times10^3$. Series representation: — —, one term; —, two term.

by Jodlbauer (1933) for air are shown on figures 1–4. The agreement is satisfactory. Particularly significant is the fact that a one-term expansion represents the temperature field rather well at up to 150° from the stagnation point. The average Nusselt number (averaged over the perimeter of the circle) is calculated as follows. Since, for the circular cylinder,

$$\xi(\pi) = \int_0^{\pi} (\sin x)^{\frac{1}{3}}\, dx = \sqrt{(\pi)}\, \frac{\Gamma(\frac{2}{3})}{\Gamma(\frac{7}{6})} \doteq 2{\cdot}59, \tag{27}$$

we have

$$\overline{\mathrm{Nu}}\, \mathrm{Gr}^{-\frac{1}{4}} = -(\tfrac{3}{4})^{\frac{1}{4}}(\tfrac{4}{9})\frac{[\xi(\pi)]^{\frac{3}{4}}}{\pi} T_0'(0) - (\tfrac{3}{4})^{\frac{1}{4}}(\tfrac{4}{9})\frac{[\xi(\pi)]^{\frac{9}{4}}}{\pi} T_1'(0)$$

$$= 0{\cdot}298 + 0{\cdot}004 = 0{\cdot}302.$$

When the characteristic length is taken as the radius, Jodlbauer's data give an average value for $\overline{\mathrm{Nu}}\, \mathrm{Gr}^{-\frac{1}{4}}$ 9 % higher. The numerical solution for a Prandtl number of 1760 gave 2·84 as a one-term approximation for $\overline{\mathrm{Nu}}\, \mathrm{Gr}^{-\frac{1}{4}}$, while the experimental value obtained by Schütz (1963) was 2·83. The table shown below is a summary of the numerical results obtained for round-nosed cylinders, $K_0 = \frac{3}{4}$, $\alpha = \frac{3}{2}$.

Pr = 0·01		Pr = 0·7		Pr = 1000	
$F_0''(0)$	$-T_0'(0)$	$F_0''(0)$	$-T_0'(0)$	$F_0''(0)$	$-T_0'(0)$
1·169	0·0593	0·8593	0·3702	0·1954	3·058

Further details are given by Saville (1965).

Of course, as the Prandtl number increases the effects of the non-linear terms in the differential equations which necessitate the expansions decrease so that the agreement at high Prandtl numbers is expected. However, as the Prandtl number tends to zero, the importance of the non-linear terms increases. Thus, it is expected that the error resulting from one-term approximations would increase. Nevertheless, at a Prandtl number of 0·01, the second term in the expansion for the average Nusselt number or shear stress was found to be less than 5 % of the first term, in the case of the circular cylinder. These 'corrections' may not always be small since the size of the 'correction' depends on the body contour for the particular body shape in question (i.e. $T(\xi, \eta) = T_0(\eta) + K_1 t_1(\eta)\xi^{\alpha} + \ldots$).

Finally, we compare the one-term approximations developed here with one- and two-term expansions of the Blasius type, as developed for free convection by Chaing & Kaye (1962) and Chaing *et al.* (1964). For a Prandtl number of 0·7 the following results were obtained for $\overline{\mathrm{Nu}}\, \mathrm{Gr}^{-\frac{1}{4}}$: for the cylinder 0·298 as compared with 0·370 and 0·317 with one- and two-term Blasius-type expansions; for the sphere 0·353 as compared with 0·458 and 0·358.

It may be noted that the differential equations and boundary conditions for the zero-order terms in the Goertler representation are the same as for the Blasius representation; thus the difference at this level is solely in the interpretation of the independent and dependent variables. The calculations for the higher-order terms have not been carried out to a degree which would determine whether or not the two types of series converge to the same limit. However, in the case of the circular cylinder, the ratio of the magnitude of the first-order term to the zero-

order term in the series for the average Nusselt number is 0·013 for the Goertler representation and 0·14 for the Blasius representation. As a consequence of this and the agreement with experimental data, one-term approximations of the Goertler type appear to be the more accurate ones.

REFERENCES

Acrivos, A. 1962 *J. Fluid Mech.* **12**, 337.

Braun, W. H., Ostrach, S. & Heighway, J. E. 1961 *Int. J. Heat Mass Transfer* **2**, 121.

Chaing, T. & Kaye, J. 1962 *Proc. 4th National Congress Appl. Mech. (Berkeley)*, p. 1213.

Chaing, T., Ossin, A. & Tien, C. L. 1964 *J. Heat Transfer*, C**86**, 537.

Goertler, H. 1957 *J. Math. Mech.* **6**, 1.

Jodlbauer, K. 1933 *Forsch. Ing.-Wes.* **4**, 157.

Hellums, J. D. & Churchill, S. W. 1960 *Chem. Eng. Progr. Symposium Series* no. **32**, **57**, 75.

Lefevre, E. J. 1957 *Proc. 9th International Congress Appl. Mech. (Brussels)* **4**, 168.

Mangler, W. 1948 *ZAMM* **28**, 97.

Merk, H. J. & Prins, J. A. 1954 *Appl. Sci. Res.* **44**, 11, 195, 207.

Morgan, G. W. & Warner, H. W. 1956 *J. Aero. Sci.* **23**, 937.

Ostrach, S. 1953 *NACA TR*, 1111.

Saville, D. A. 1965 Ph.D. Thesis, University of Michigan, Ann Arbor, Mich.

Schmidt, E. & Beckmann, W. 1930 *Tech. Mech. Thermodynamik* **1**, 341, 391.

Schütz, G. 1963 *Int. J. Heat Mass Transfer* **6**, 873.